Supplementary information, Data S1

Methods and Meterials

Cloning, Expression and Purification

The gene encoding full-length human Pannexin-1 (Uniprot code: Q96RD7) was synthesized (Genscripts) with codon optimized for *Homo sapiens* and was cloned into a BacMam expression vector. For protein purification, decahistidine tag was added at C-terminus of the gene before amber code with a short linker peptide (GSGS). Construct with gene of full-length wild-type PANX1 was named $PANX1_{WT}$; Construct with gene of C-terminal truncated PANX1 (376-426 truncated) was named $PANX1_{\Delta C}$; Construct with anti-cleavage mutations (D376E, D379E) introduced base on $PANX1_{WT}$ was named $PANX1_{EE}$.

Recombinant baculovirus of PANX1s were generated using the Bac-to-Bac system (Invitrogen) following manufacturer's instructions. Briefly, DH10Bac cells were used to generate bacmid vectors and Sf9 cells (Invitrogen) were used for bacmids transfection to generate P1 virus. P2 and P3 virus were then generated stepwise by infecting cells with the previous generation virus at a MOI of 0.05. For large-scale expression, HEK293F cells (ATCC) growing in SMM 293-TI (Sino Biological Inc.) supplemented with 2% FBS (Gibco), 2 mM GlutaMAX-I (Gibco) were infected with P3 virus at a ratio of 1:10 (virus:HEK293F, v:v) and expression level was further boosted by adding 10 mM sodium butyrate (Sigma-Aldrich). Cells were cultured at 37°C, 8% CO_2 for 48 hr before harvest.

The cell pellet was resuspended lysis buffer (50 mM HEPES, 150 mM NaCl, pH 7.5, supplement with 2 μg/ml DNase I, 2 μg/ml pepstatin, 2 μg/ml leupeptin, 2 μg/ml aprotinin and 1 mM PMSF) and homogenized by sonication on ice. The membrane fraction was collected by high-speed centrifugation (10,000 g for 30 min) followed ultracentrifugation (100,000 g for 1 hr) and the pellet was mechanically homogenized and solubilized in extraction buffer (50 mM HEPES-NaOH, 150 mM NaCl, 2% (w:v) decyl maltose neopentyl glycol (DMNG, Anatrace) and 0.2% (w:v) cholesteryl hemisuccinate (CHS, Anatrace), pH 7.5) for 3 hr along with gentle agitation. Solubilized PANX1 was separated by high speed centrifugation (48,000 g for 30 min) and the supernatant was supplemented with 20 mM imidazole, mixed with Talon Co^{2+} affinity resin (Clontech) pre-equilibrated with SEC buffer (50 mM HEPES, 150 mM NaCl and 0.05 mM lauryl maltose neopentyl glycol (LMNG, Anatrace), pH 7.5) and was incubated overnight under gentle agitation. The resin was collected on a disposable gravity column (Bio-Rad), washed with SEC buffer supplement with 20 mM imidazole for 16 column volumes. PANX1 was eluted with SEC buffer supplement with 300 mM imidazole and was further purified by size exclusion chromatography on a Superose 6 10/300 GL column (GE Healthcare) pre-equilibrated with SEC buffer. The peak fractions were pooled, concentrated to 4-5 mg/ml using a spin concentrator 100-kD cutoff (Millipore) for cryo-electron microscopy analysis. For $PANX1_{CBX}$ purification, 100 μM CBX was supplied from homogenization.

Nanodiscs Reconstitution

For $PANX1_{WT}$ nanodiscs reconstitution, protein was purified as described above except the detergents DMNG and LMNG were exchanged with n-Dodecyl-β-D-Maltopyranodise (DDM, Anatrace). After size exclusion chromatography, the protein peak fractions were pooled, concentrated to 75 μM and were mixed with 25 mM soybean polar lipid extract (Avanti) stock in 3% (w:v) DDM at a ratio of 4:1 (v:v), incubated with gentle agitation for 1 hr. The protein-lipids mixture was further mixed with 90 μM MSP1E3D1 (Addgene #20066) at a ratio of 1:1 (v:v), resulting in a final PANX1:MSP1E3D1:Lipids monomer ratio of 1:1.5:75, and was equilibrated for another 30 min. Detergents were removed by adding Bio-Beads SM2 (Bio-Rad) to a concentration of 20 mg/ml with gentle agitation for 2 hr followed by Bio-Beads supplement to a final concentration of 100mg/ml. The used Bio-Beads were replaced with fresh ones every 8 hr for six times. Afterwards, the sample was filtered with a disposable gravity column and reconstituted PANX1 nanodiscs was separated on a Superose 6 10/300 GL column pre-equilibrated with 50 mM HEPES pH 7.5, 150 mM NaCl. The peak fractions were pooled, concentrated to ~1.5 mg/ml for cryo-electron microscopy analysis.

Cryo-EM Sample Preparation and Data Acquisition

3.5 μL of purified protein (either in detergents or reconstituted into nanodiscs) was pipetted onto a glow-discharged Quantifoil R 1.2/1.3 300-mesh copper holey carbon grid (Quantifoil). Grids were blotted for 3 s with a blotting force of -3 and a humidity

of 100% at 4℃ and flash frozen into liquid nitrogen cooled liquid ethane using an Mark IV Vitrobot (FEI). Micrographs were acquired on an Titan Krios microscope (FEI) operated at 300 kV and equipped with a GIF-Quantum energy filter operated with a 20 eV energy slit with an K2 Summit direct electron detector camera (Gatan) set to super-resolution counting mode. SerialEM software[1] (FEI) was used for automated data collection following standard FEI procedure. For the data of $PANX1_{WT}$, $PANX1_{EE}$ and $PANX1_{ND}$, images were recorded at a normal magnification of 130,000 X, corresponding to a pixel size of 1.055 Å per pixel and with a set defocus range of 1.5 to 2.5 μm. Each micrograph was dose-fractionated to 32 frames recorded every 0.25 s under a dose rate of 8 e^-/pixel/s, resulting in an accumulated dose of ~57.5 e^-/Å. For the data of $PANX1_{CBX}$, images were recorded at a normal magnification of 130,000 X, corresponding to a pixel size of 1.080 Å per pixel and with a set defocus range of 1.5 to 2.5 μm. Each micrograph was dose-fractionated to 32 frames recorded every 0.24 s under a dose rate of 10 e^-/pixel/s, resulting in an accumulated dose of ~65.6 e^-/Å.

Cryo-EM Data Processing

Data processing for $PANX1_{EE}$, a total of 5397 movies were collected, aligned, and does-weighted to correct for movement during imaging and account for radiation damage via Motioncor2[2]. The CTF parameters for each micrograph were determined by Gctf[3]. Manual particle picking (~2,000 particles) and reference-free 2D

classification were carried out to generate templates for automated particle picking in CryoSPARC v2[4]. A total of 869835 particles were autopicked and subjected to several rounds of reference-free 2D classification followed by manual inspection and selection of classes with transmembrane helix like features. This process yielded a stack of 340575 cleaned particles that were subjected to per-particle local motion correction, then 2D classification and ab initio 3D reconstruction classification in cryoSPARC V2[4], the most representative class and associate particles are taken for further refinement. Homogenous 3D refinement in C7 symmetry, followed with the non-uniform and local refinement as implemented in cryoSPARC V2 workflow, yielded final maps to a resolution of 3.6 Å (0.143 FSC). Local resolution estimation is also performed in cryoSPARC V2[4]. Data processing for $PANX1_{WT}$, $PANX1_{CBX}$ and $PANX1_{ND}$ are same as that for $PANX1_{EE}$. Diagrams of the procedures used in data processing are presented in Supplementary information Figure S2-S5.

Model Building, Refinement and Validation

De novo atomic model building based on 3.6 Å resolution density map of $PANX1_{EE}$ was performed in Coot[5]. Amino acid assignment was achieved based on the clearly defined density for two pairs of disulfate bond and bulky residues (Phe, Trp, Tyr, Arg) on E1H and four transmembrane helices. Models were refined against summed maps using phenix.real_space_refine[6], with secondary structure restraints and non-crystallography symmetry applied, and re-adjusted in Coot[5], iteratively, until no

further improvement in model geometry could be obtained. The initial EM density map allowed us to construct a PANX1 model containing residues 35-156 and 195-336.

For the models of $PANX1_{WT}$ and $PANX1_{CBX}$, the atomic model of $PANX1_{EE}$ was fitted into the 3D density maps using UCSF Chimera[7] and applied to refinement using phenix.real_space_refine[6] and Coot[5] as mentioned above. The statistics for the geometries of models was generated using MolProbity[8] and summarized in supplementary information Table S1.

The structure comparisons among different models of PANX1, or between PANX1 and other similar proteins including cINX6 (PDB: 5H1Q) and mLRRC8A (PDB: 6G8Z), were processed using CCP4i2[9]. All the figures of models were prepared in PyMol and all the figures of density maps were prepared in UCSF Chimera[7].

ATP Release Assay

Extracellular ATP was measured by the luciferin-luciferase reaction. Briefly, HEK293T cells (ATCC) were grew in 24-well plates (Corning Costar) to 70% and were transiently transfected with either empty vector or PANX1 vectors using lipofectamine 2000 transfection regents (Invitrogen). Transfected cells were wash with NaCl buffer (140 mM NaCl, 3 mM KCl, 1.5 mM Na2HPO4, 1 mM MgSO4, 2 mM CaCl2, 10 mM Glucose and 10mM HEPES-NaOH (pH7.4)) twice 16 hr after transfection and were incubated in either NaCl buffer or KCl buffer (143 mM KCl, 1.5 mM Na2HPO4, 1 mM MgSO4, 2 mM CaCl2, 10 mM Glucose and 10mM

HEPES-NaOH (pH7.4)) for 1 hr. Supernatants were then transferred to a 96-well microplate (Corning Costar) and mixed with CellTiter-Glo luminescent cell viability assay solution (Promega) with a ratio of 2:1 (v:v). ATP concentration was calculated from reading luminance according to pre-generated ATP standard curve.

To measure the effects of hypotonic conditions on ATP release of PANX1, HEK293T cells were grew in 24-well plates to 70% and were transiently transfected with either empty vector or PANX1 vectors using lipofectamine 2000 transfection regents. Transfected cells were wash with NaCl buffer (140 mM NaCl, 3 mM KCl, 1.5 mM Na2HPO4, 1 mM MgSO4, 2 mM CaCl2, 10 mM Glucose and 10mM HEPES-NaOH (pH7.4)) twice 16 hr after transfection and were incubated in different NaCl buffer with different concentration of NaCl (143 mM KCl, 1.5 mM Na2HPO4, 1 mM MgSO4, 2 mM CaCl2, 10 mM Glucose and 10mM HEPES-NaOH (pH7.4)) for 1 hr. 140N means cells treated with solution containing 140 mM NaCl, 3 mM KCl, 1.5 mM Na2HPO4, 1 mM MgSO4, 2 mM CaCl2, 10 mM Glucose and 10mM HEPES-NaOH (pH7.4). 120N means cells treated with solution containing 120 mM NaCl, 3 mM KCl, 1.5 mM Na2HPO4, 1 mM MgSO4, 2 mM CaCl2, 10 mM Glucose and 10mM HEPES-NaOH (pH7.4). 100N means cells treated with solution containing 100 mM NaCl, 3 mM KCl, 1.5 mM Na2HPO4, 1 mM MgSO4, 2 mM CaCl2, 10 mM Glucose and 10mM HEPES-NaOH (pH7.4). 80N means cells treated with solution containing 80 mM NaCl, 3 mM KCl, 1.5 mM Na2HPO4, 1 mM MgSO4, 2 mM CaCl2, 10 mM Glucose and 10mM HEPES-NaOH (pH7.4). Supernatants were measured with CellTiter-Glo luminescent cell viability assay.

To measure the inhibitory effect of CBX (Abcam) on ATP release of PANX1. HEK293T cells were grew in 24-well plates to 70% and were transiently transfected with either empty vector or $PANX1_{\Delta C}$ vectors using lipofectamine 2000 transfection regents. Transfected cells were incubated with 25 mM trovafloxacin (Trovan, MCE) to prevent death effect of truncated PANX1 on HEK293T cells. After 16hr, cells were wash with NaCl buffer supplement with or without 100 μM CBX for 1 hr. Supernatants were measured with CellTiter-Glo luminescent cell viability assay.

Statistical Analysis

Unless otherwise specified, ATP release assay was repeated three times. Error bars represent SEM. Regression and statistical analyses were carried out with the computer program OriginPro 2019 (OriginLab). Differences in mean values of paired samples were evaluated with the Student's t-test.

References

1. Mastronarde, D. N. Automated electron microscope tomography using robust prediction of specimen movements. *J. Struct. Biol.* **152**, 36-51 (2005).
2. Zheng, S. Q. et al. MotionCor2: anisotropic correction of beam-induced motion for improved cryo-electron microscopy. *Nat. Methods* **14**, 331-332 (2017).
3. Zhang, K. Gctf: Real-time CTF determination and correction. *J. Struct. Biol.* **193**, 1-12 (2016).
4. Punjani, A., Rubinstein, J. L., Fleet, D. J. & Brubaker, M. A. cryoSPARC: algorithms for rapid unsupervised cryo-EM structure determination. *Nat. Methods* **14**, 290-296 (2017).
5. Emsley, P., Lohkamp, B., Scott, W. G. & Cowtan, K. Features and development of Coot. *Acta Crystallogr. D Biol. Crystallogr.* **66**, 486-501 (2010).
6. Liebschner, D. et al. Macromolecular structure determination using X-rays, neutrons and electrons: recent developments in Phenix. *Acta Crystallogr. D Struct. Biol.* **75**, 861-877 (2019).

7. Pettersen, E. F. et al. UCSF chimera - A visualization system for exploratory research and analysis. *J. Comput. Chem.* **25**, 1605-1612 (2004).
8. Chen, V. B. et al. MolProbity: all-atom structure validation for macromolecular crystallography. *Acta Crystallogr. D Biol. Crystallogr.* **66**, 12-21 (2010).
9. Potterton, L. et al. CCP4i2: the new graphical user interface to the CCP4 program suite. *Acta Crystallogr. D Struct. Biol.* **74**, 68-84 (2018).

Supplementary information, Table S1

	$PANX1_{WT}$	$PANX1_{EE}$	$PANX1_{CBX}$	$PANX1_{ND}$
Data collection and processing				
Magnification	47388.8	47388.8	46296.3	47388.8
Voltage (kV)	300	300	300	300
Electron exposure (e–/Å^2)	~57.5	~57.5	~65.8	~57.5
Defocus range (μm)	-1.5 to -2.5	-1.5 to -2.5	-1.5 to -2.5	-1.5 to -2.5
Pixel size (Å)	0.528(Super–resolution)	0.528(Super–resolution)	0.540(Super–resolution)	0.528(Super–resolution)
Symmetry imposed	*C7*	*C7*	*C7*	*C7*
Initial particle images	4869	5397	1651	5705
Final particle images	4347	4461	1363	1957
Map resolution (Å)	4.1	3.6	4.6	6.6
FSC threshold	0.143	0.143	0.143	0.143
Refinement				
Model resolution (Å)	4.1	3.6	4.3	
Map sharpening B factor (Å^2)	-158.6	-158.6	-158.6	
Model composition				
Non-hydrogen atoms	14938	14938	14938	
Protein residues	1855	1855	1855	
Ligands	0	0	0	
r.m.s. deviation				
Bond lengths (Å)	0.005	0.006	0.006	
Bond angles (°)	1.073	1.134	1.079	
Validation				
MolProbity score	2.01	1.93	1.78	
Clashscore	9.42	6.79	4.45	

Rotamer outliers (%)	0.00	0.00	0.00
Ramachandran plot			
Favored (%)	91.19	89.66	89.66
Allowed (%)	8.81	10.34	10.34
Outliers (%)	0.00	0.00	0.00

Supplementary information, Figures

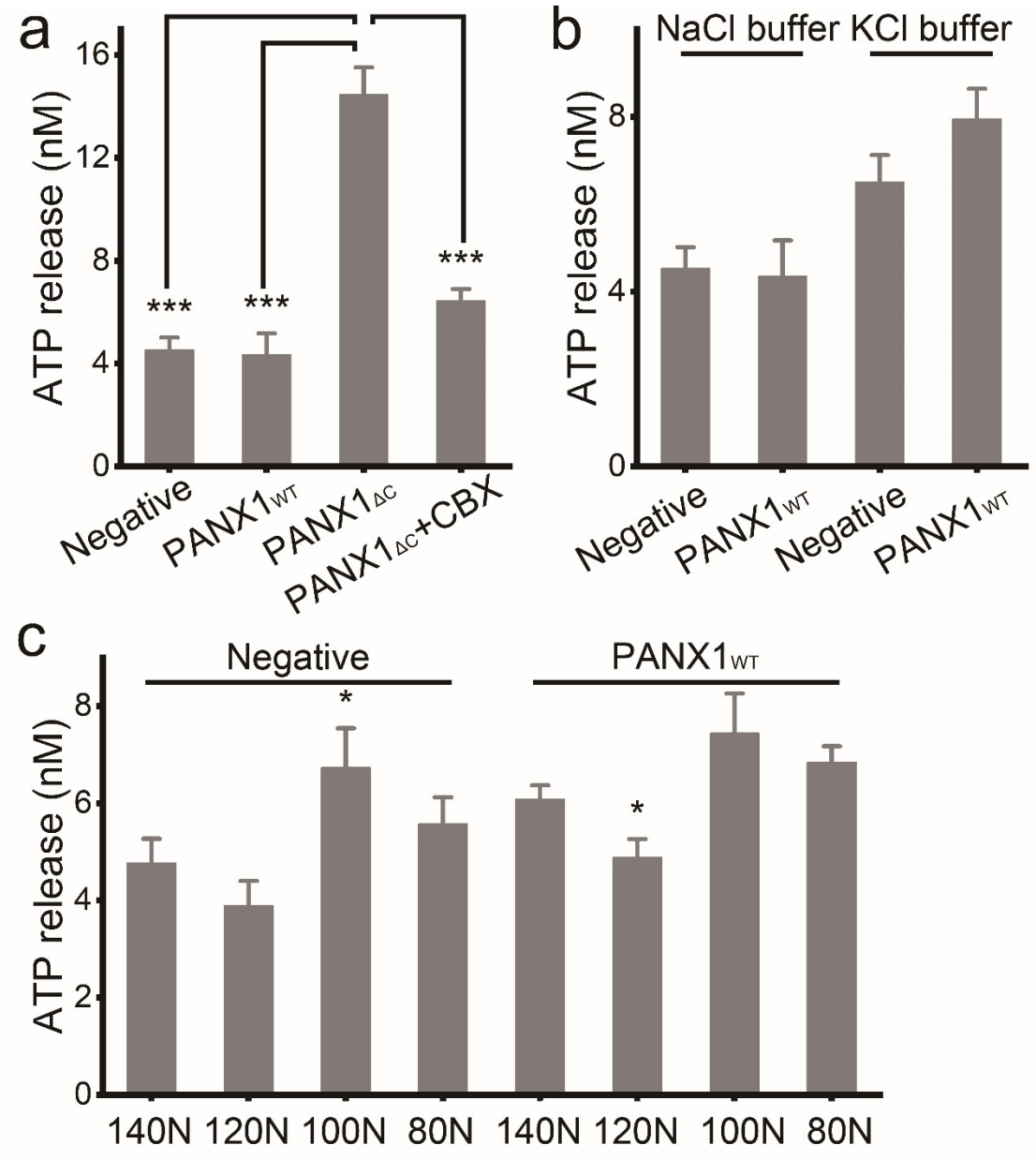

Figure S1. Functional characterization of PANX1 in HEK293T cell. **a** ATP releasing assay of HEK293T cells expressing $PANX1_{WT}$, $PANX1_{\Delta C}$ or empty vector treated with or without CBX. **b** ATP release assay of HEK293T cells expressing $PANX1_{WT}$ or empty vector treated with different concentrations of extracellular K^+. NaCl buffer contains 140 mM NaCl, 3 mM KCl, 1.5 mM Na_2HPO_4, 1 mM $MgSO_4$, 2 mM $CaCl_2$,

10 mM Glucose and 10mM HEPES-NaOH (pH7.4). KCl buffer contains 143 mM KCl, 1.5 mM Na_2HPO_4, 1 mM $MgSO_4$, 2 mM $CaCl_2$, 10 mM Glucose and 10mM HEPES-NaOH (pH7.4). **c** ATP release assay of HEK293T cells expressing $PANX1_{WT}$ or empty vector treated with different hypotonic conditions. hypotonic conditions are archived by changing the concentration of ions. For 140N means cells treated with solution containing 140 mM NaCl, 3 mM KCl, 1.5 mM Na_2HPO_4, 1 mM $MgSO_4$, 2 mM $CaCl_2$, 10 mM Glucose and 10mM HEPES-NaOH (pH7.4). 120N means cells treated with solution containing 120 mM NaCl, 3 mM KCl, 1.5 mM Na_2HPO_4, 1 mM $MgSO_4$, 2 mM $CaCl_2$, 10 mM Glucose and 10mM HEPES-NaOH (pH7.4). 100N means cells treated with solution containing 100 mM NaCl, 3 mM KCl, 1.5 mM Na_2HPO_4, 1 mM $MgSO_4$, 2 mM $CaCl_2$, 10 mM Glucose and 10mM HEPES-NaOH (pH7.4). 80N means cells treated with solution containing 80 mM NaCl, 3 mM KCl, 1.5 mM Na_2HPO_4, 1 mM $MgSO_4$, 2 mM $CaCl_2$, 10 mM Glucose and 10mM HEPES-NaOH (pH7.4).

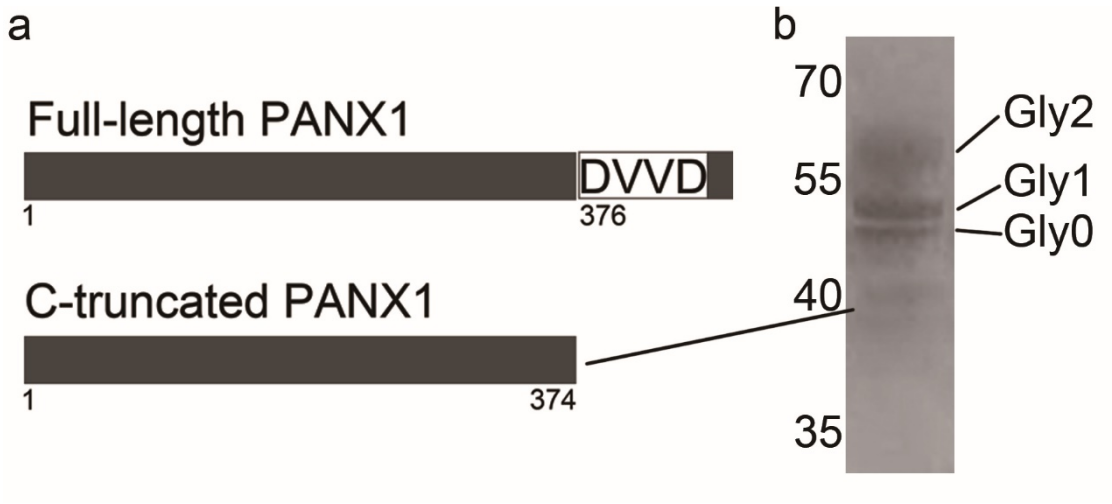

Figure S2. Purification and biochemical characterization of PANX1 channel in different states. **a** Hypothesis explaining the biochemistry results for wild-type PANX1 channel expression. **b** Representative SDS-PAGEs of PANX1WT with glycosylated states labeled.

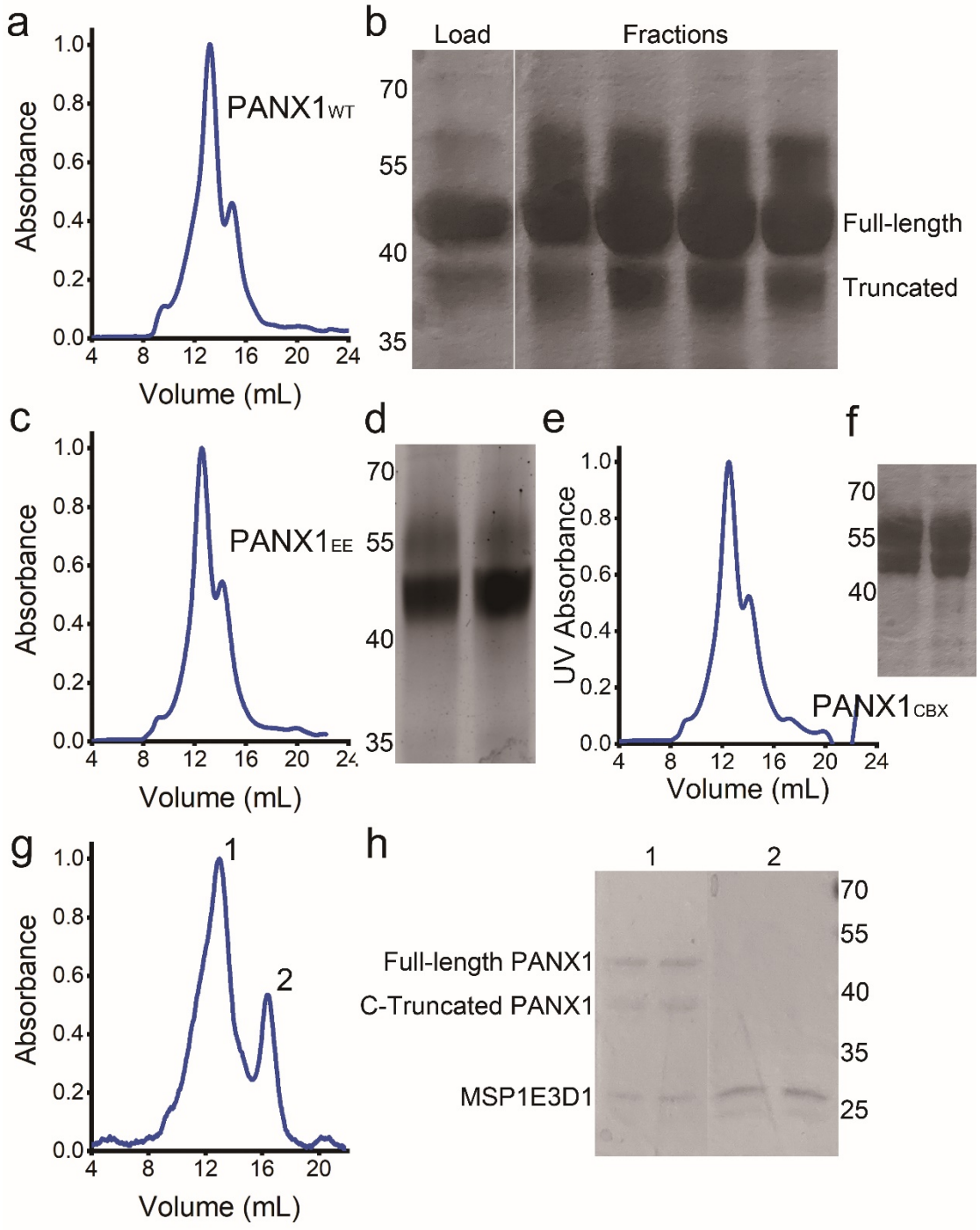

212

213 **Figure S3.** Purification and biochemical characterization of PANX1 channel in

214 different states. **a,c,e,g** Representative size-exclusion chromatography profiles of

215 PANX1WT **(a)**, PANX1EE **(c)**, PANX1CBX **(e)** or PANX1ND **(g)** on Superose 6

216 column. **b,d,f,h** Representative SDS-PAGEs of PANX1WT **(b)**, PANX1EE **(d)**,

PANX1CBX **(f)** or PANX1ND **(h)** with lanes corresponding to size-exclusion chromatography profile.

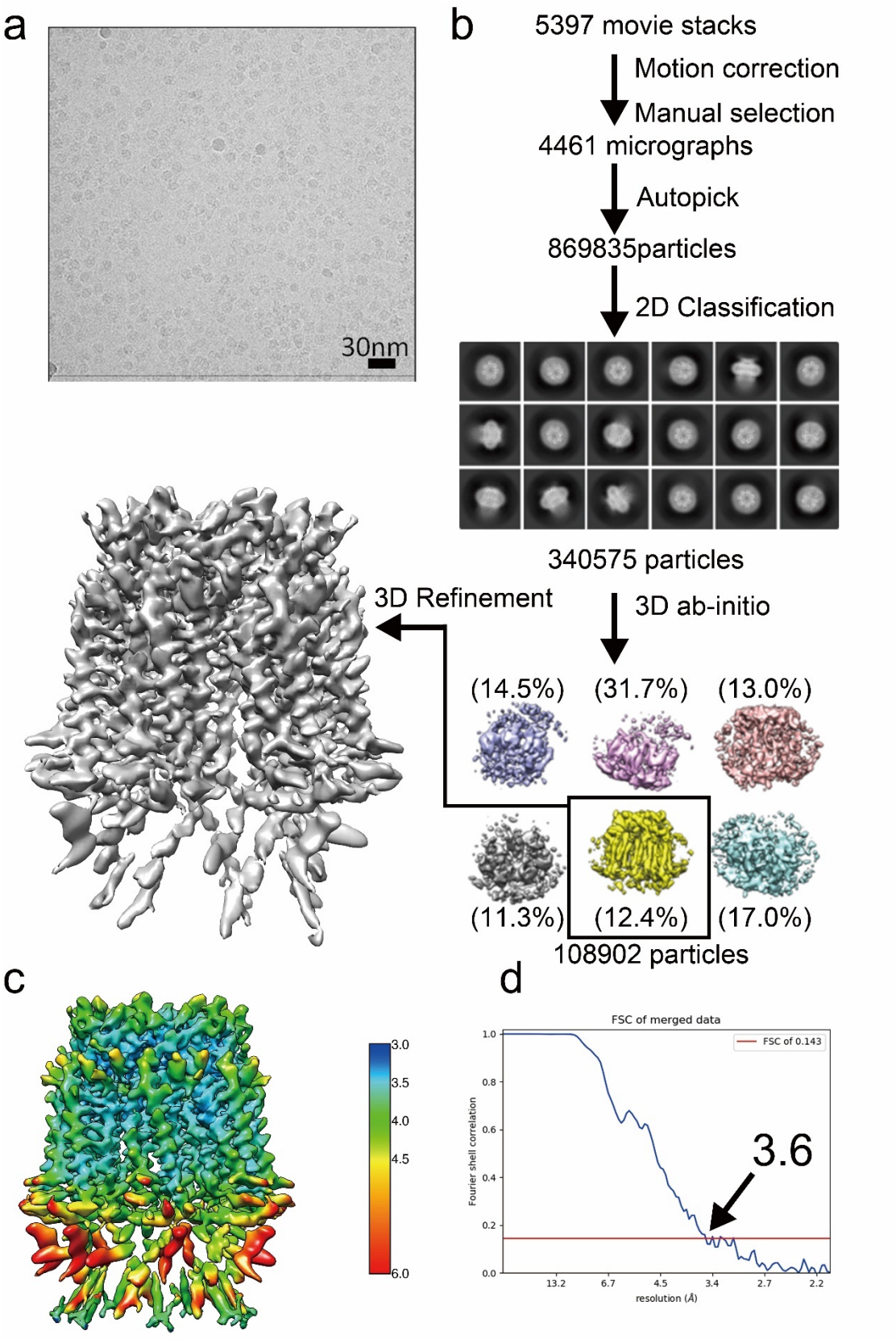

Figure S4. Structure determination of $PANX1_{EE}$. **a** Representative cryo-EM micrograph of $PANX1_{EE}$. **b** Flowchart of image processing for $PANX1_{EE}$ particles. **c**

223 The density maps of $PANX1_{EE}$ colored by local resolution. **d** Gold standard FSC curves

224 of the final 3D reconstruction.

225

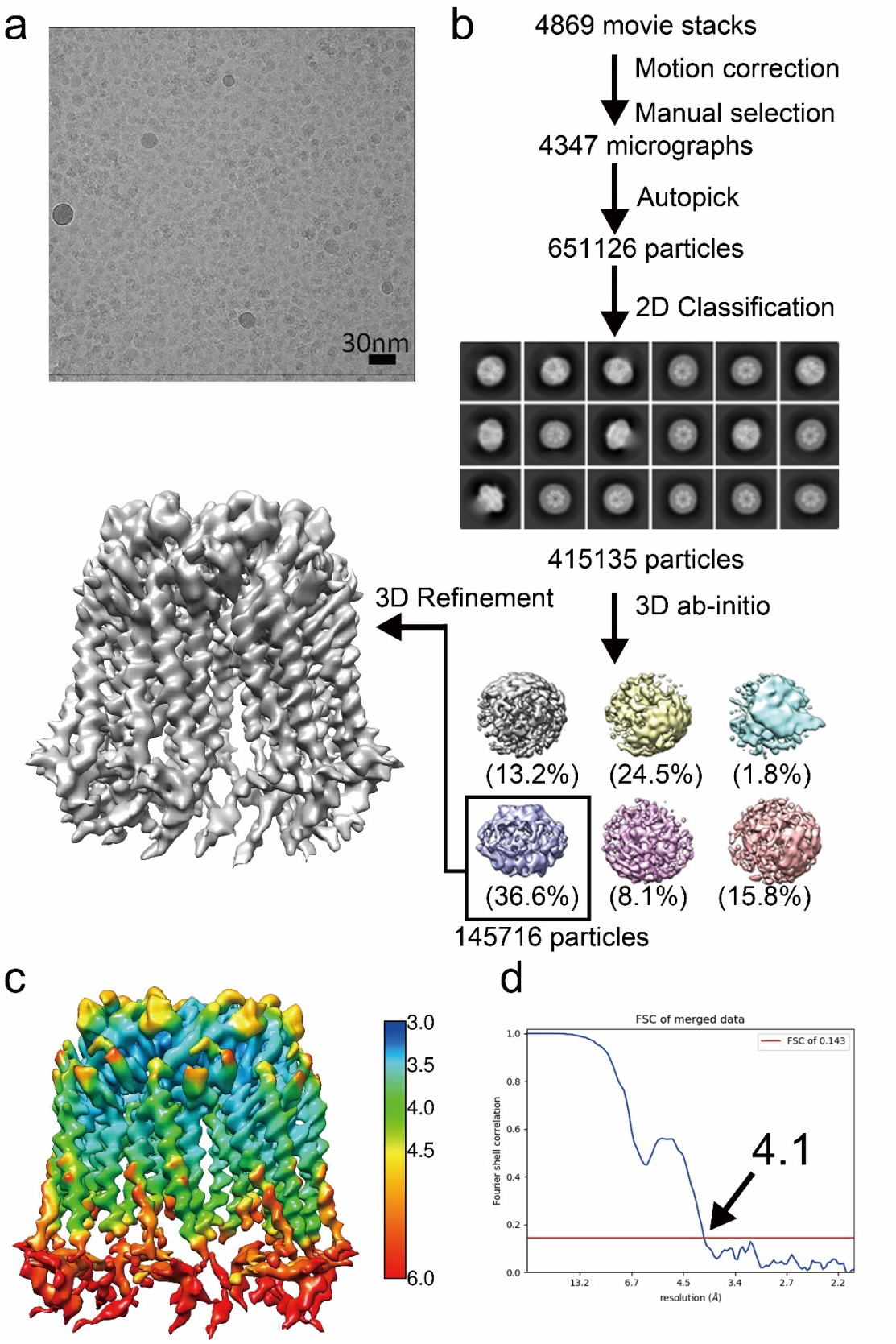

Figure S5. Structure determination of PANX1$_{WT}$. **a** Representative cryo-EM micrograph of PANX1$_{WT}$. **b** Flowchart of image processing for PANX1$_{WT}$ particles. **c**

229 The density maps of $PANX1_{WT}$ colored by local resolution. **d** Gold standard FSC curves

230 of the final 3D reconstruction.

231

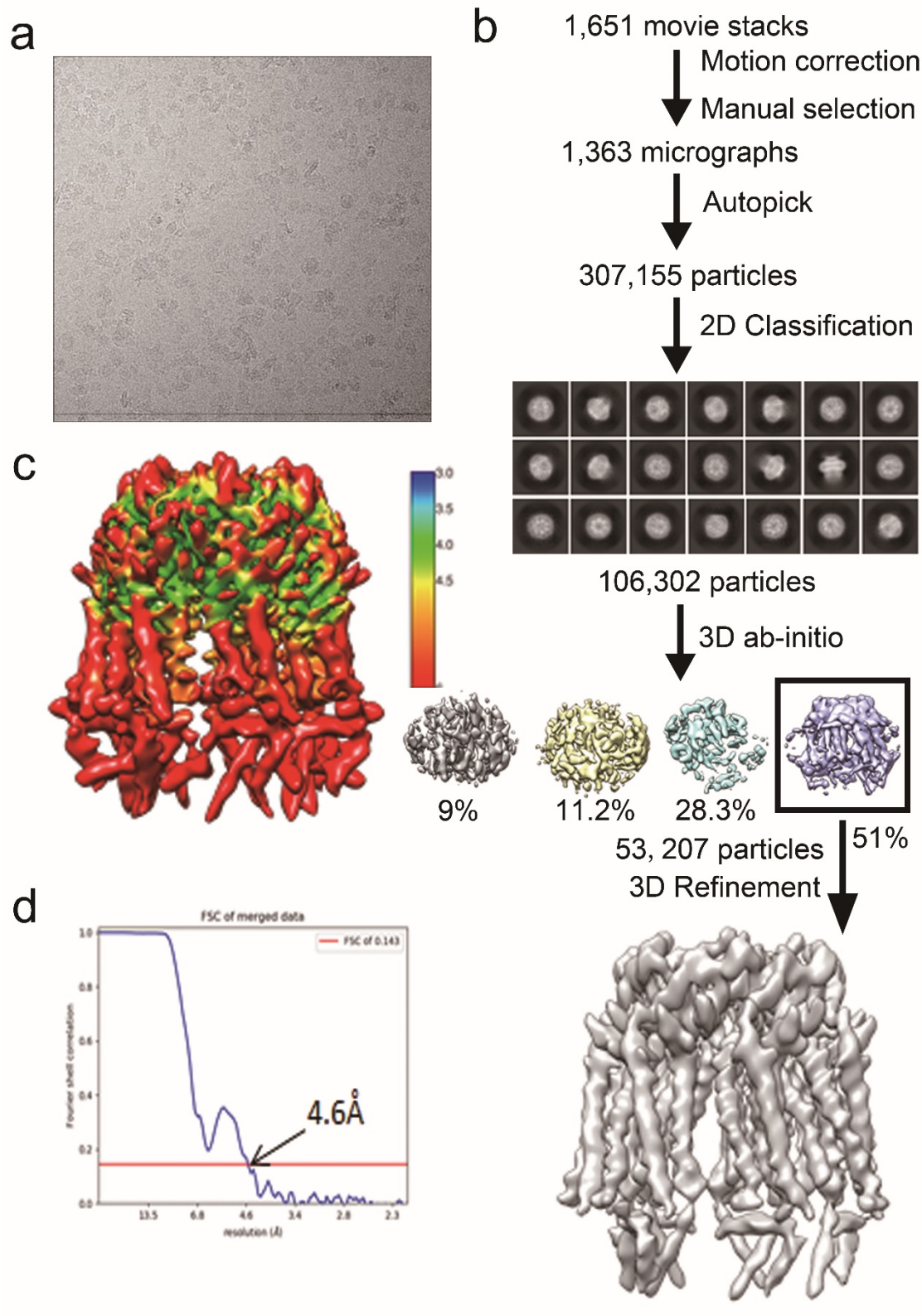

Figure S6. Structure determination of $PANX1_{CBX}$. **a** Representative cryo-EM micrograph of $PANX1_{CBX}$. **b** Flowchart of image processing for $PANX1_{CBX}$. **c** The

density maps of PANX1$_{CBX}$ colored by local resolution. **d** Gold standard FSC curves of the final 3D reconstruction.

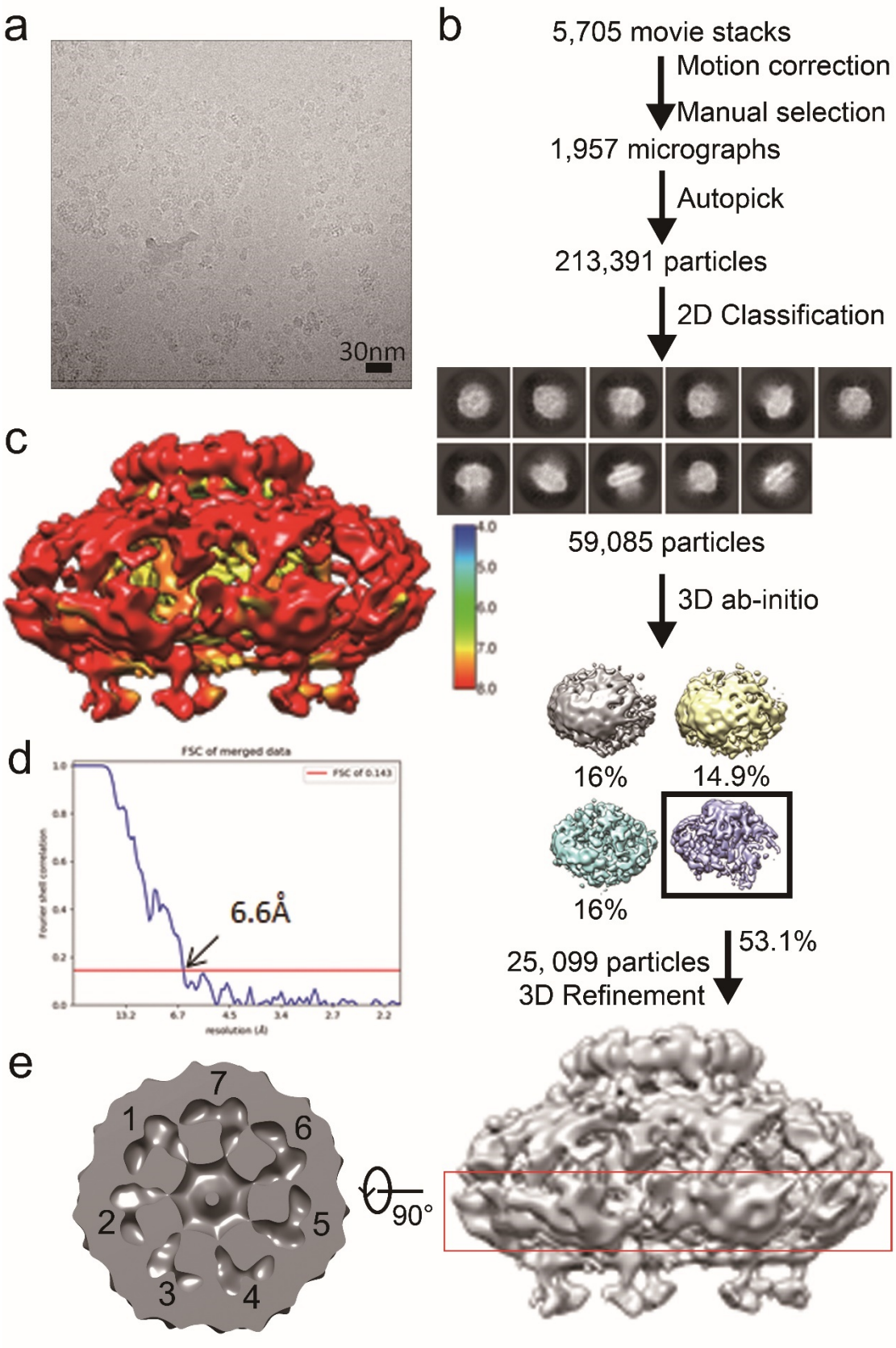
a
30nm
b
5,705 movie stacks
Motion correction
Manual selection
1,957 micrographs
Autopick
213,391 particles
2D Classification
59,085 particles
3D ab-initio
16%
14.9%
16%
25, 099 particles
3D Refinement
53.1%
c
4.0
5.0
6.0
7.0
8.0
d
FSC of merged data
FSC of 0.143
Fourier shell correlation
resolution (Å)
6.6Å
e
1
2
3
4
5
6
7
90°

Figure S7. Structure determination of $PANX1_{ND}$. **a** Representative cryo-EM micrograph of $PANX1_{ND}$. **b** Flowchart of image processing for $PANX1_{ND}$. **c** The density maps of $PANX1_{ND}$ colored by local resolution. **d** Gold standard FSC curves of the final 3D reconstruction. **e** The cross section of $PANX1_{ND}$ density map with each subunit numbered.

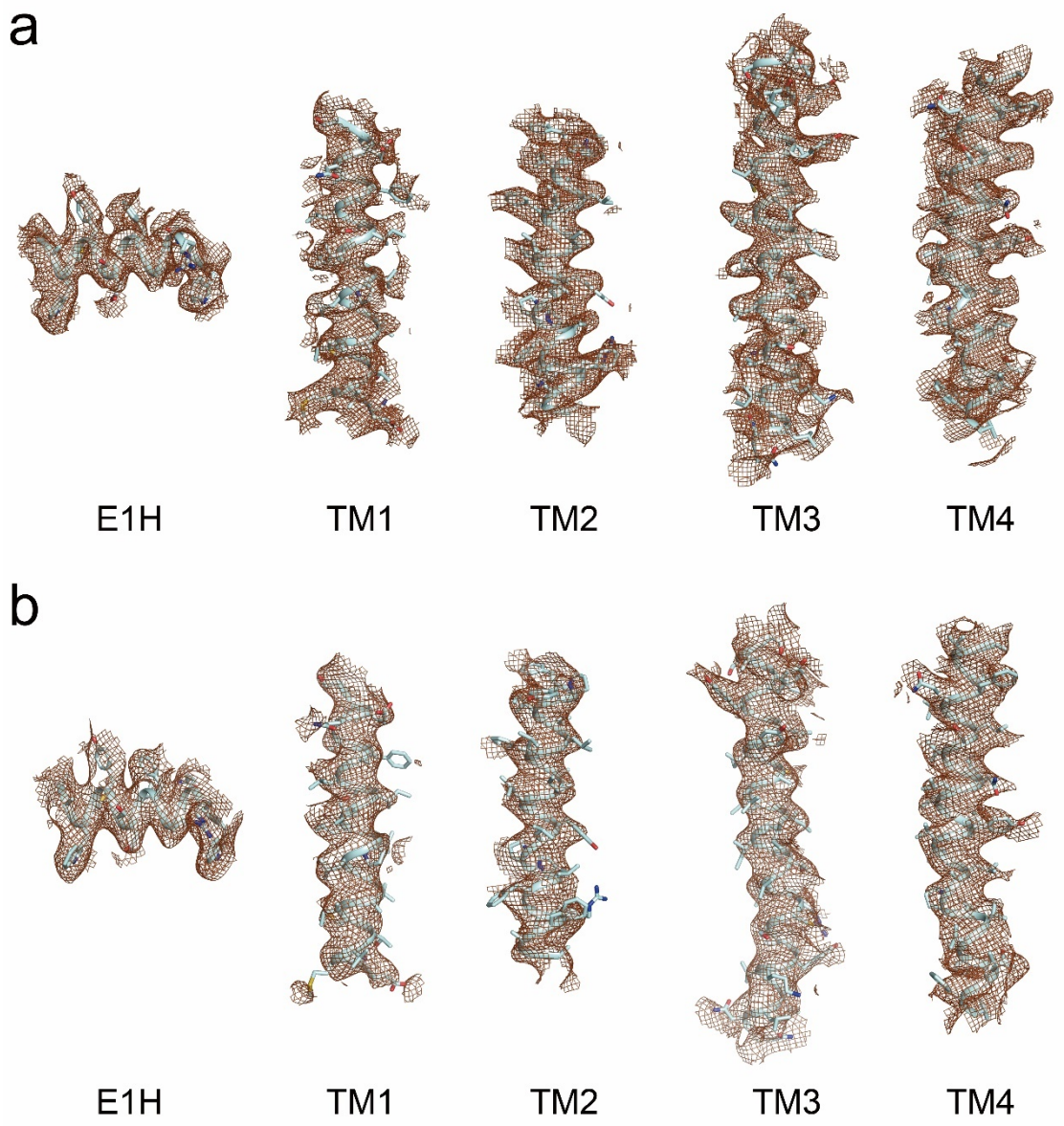

Figure S8. Cryo-EM density maps of $PANX1_{EE}$ and $PANX1_{WT}$. **a** Sample maps at 4 transmembrane helices and intracellular helix of $PANX1_{EE}$. **b** Sample maps at 4 transmembrane helices and intracellular helix of $PANX1_{WT}$. The maps are low-pass filtered to 4.1 Å for map of $PANX1_{WT}$ and 3.6 Å for the map of $PANX1_{EE}$. All the maps are sharpened with a temperature factor of -158.6 Å2.

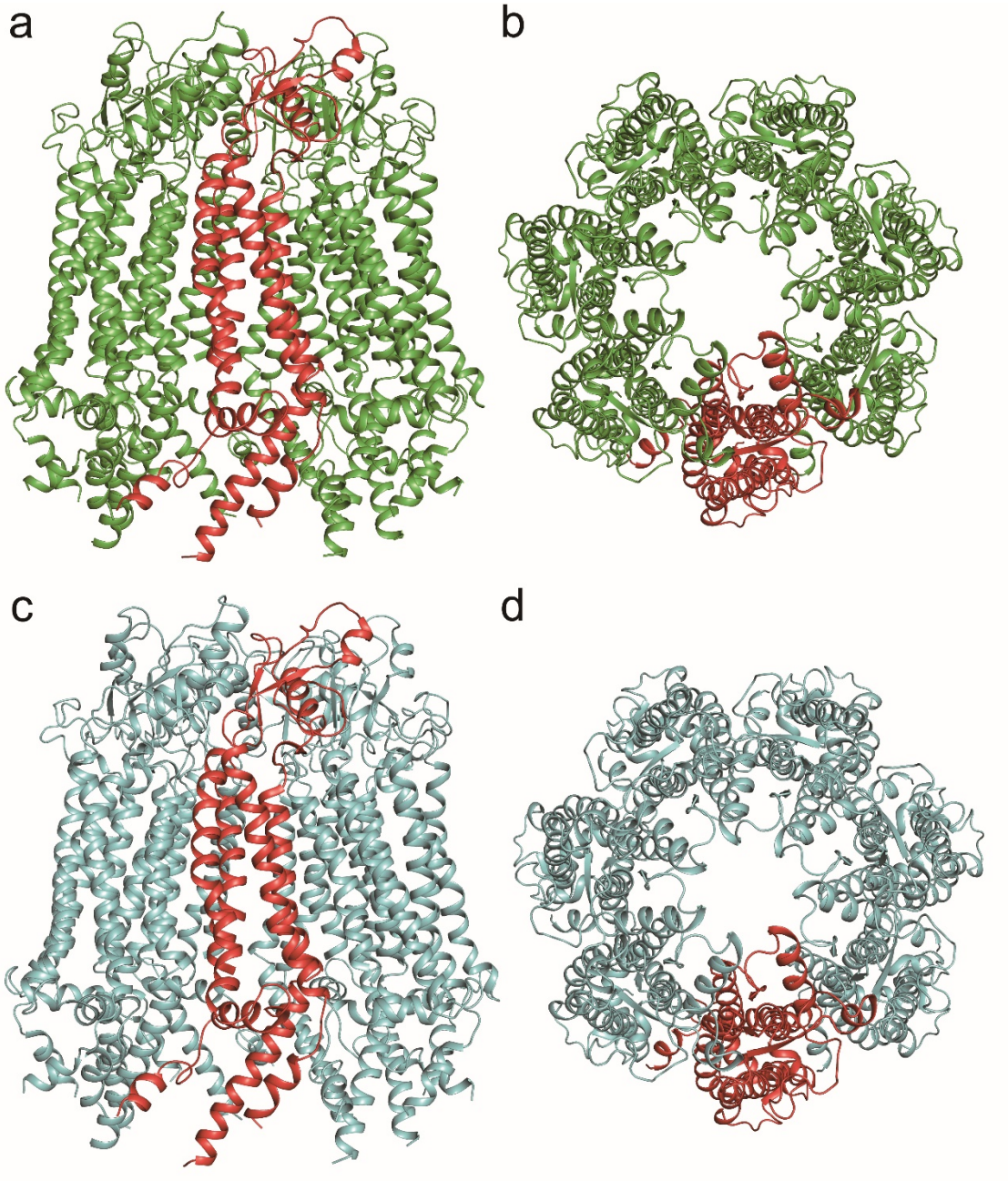

Figure S9. Structures of $PANX1_{WT}$ and $PANX1_{CBX}$. **a,b** Ribbon representations of $PANX1_{WT}$ structure viewed parallel to the plasma membrane **(a)** or from the extracellular side down the seven-fold symmetry axis **(b)**. **c,d** Ribbon representations of $PANX1_{CBX}$ structure viewed parallel to the plasma membrane **(c)** or from the extracellular side down the seven-fold symmetry axis **(d)**.

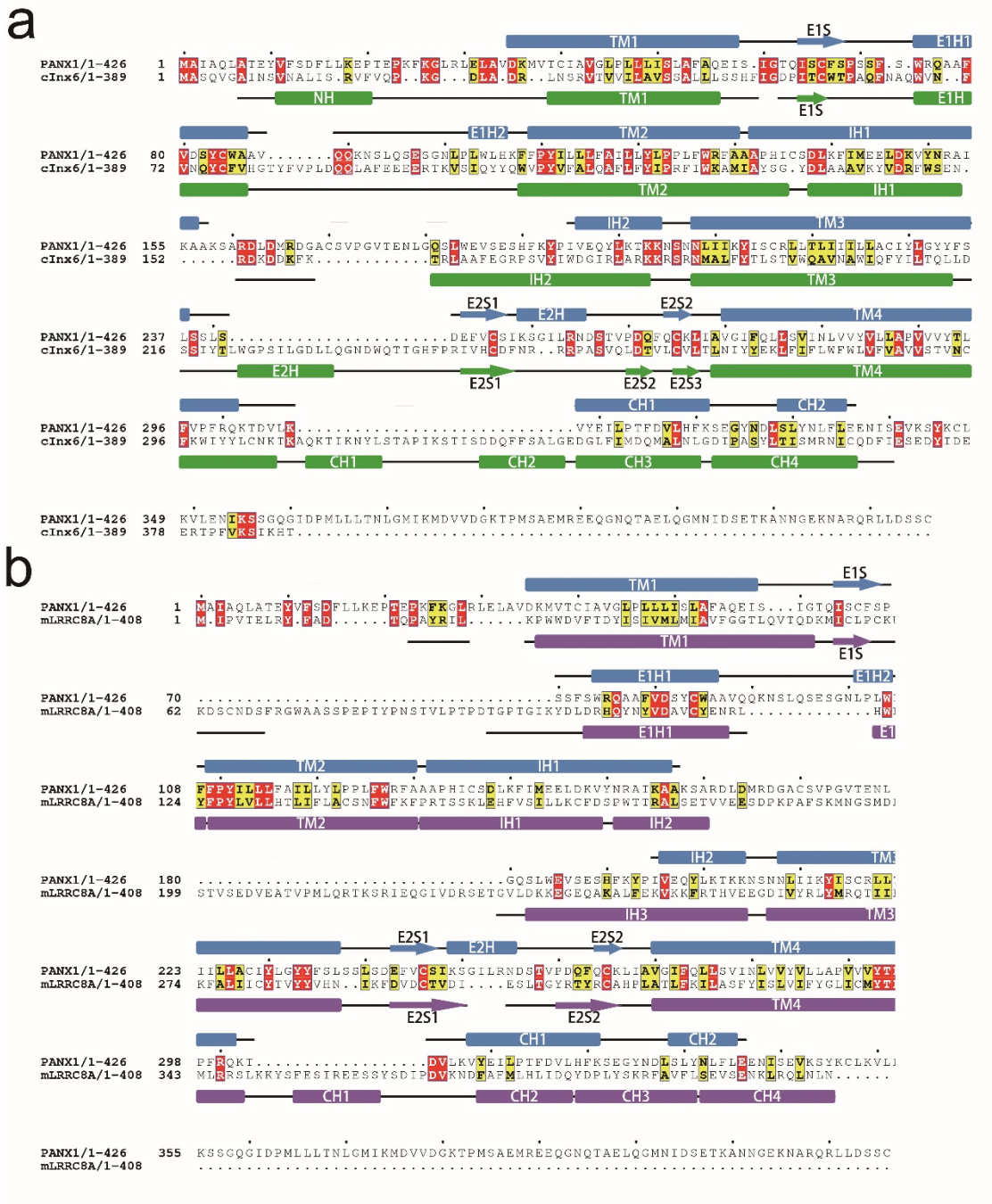

Figure S10. Sequence alignments between PANX1 and other large pore-forming channels. **a** Structural based sequence alignment of human PANX1 (UniProt: Q96RD7) and *c.elegans* INX6 (UniProt: Q9U3N4, PDB: 5H1Q). Identical residues are colored in red and similar residues are colored in yellow. Residues assigned in the structure are labelled with black lines and secondary structures are additionally labelled in blue for

PANX1 and green for cINX6. **b** Structural based sequence alignment of human PANX1 (UniProt: Q96RD7) and *m.musculus* LRRC8A (UniProt: Q80WG5, PDB: 6G8Z). Identical residues are colored in red and similar residues are colored in yellow. Residues assigned in the structure are labelled with black lines and secondary structures are additionally labelled in blue for PANX1 and purple for mLRRC8A.

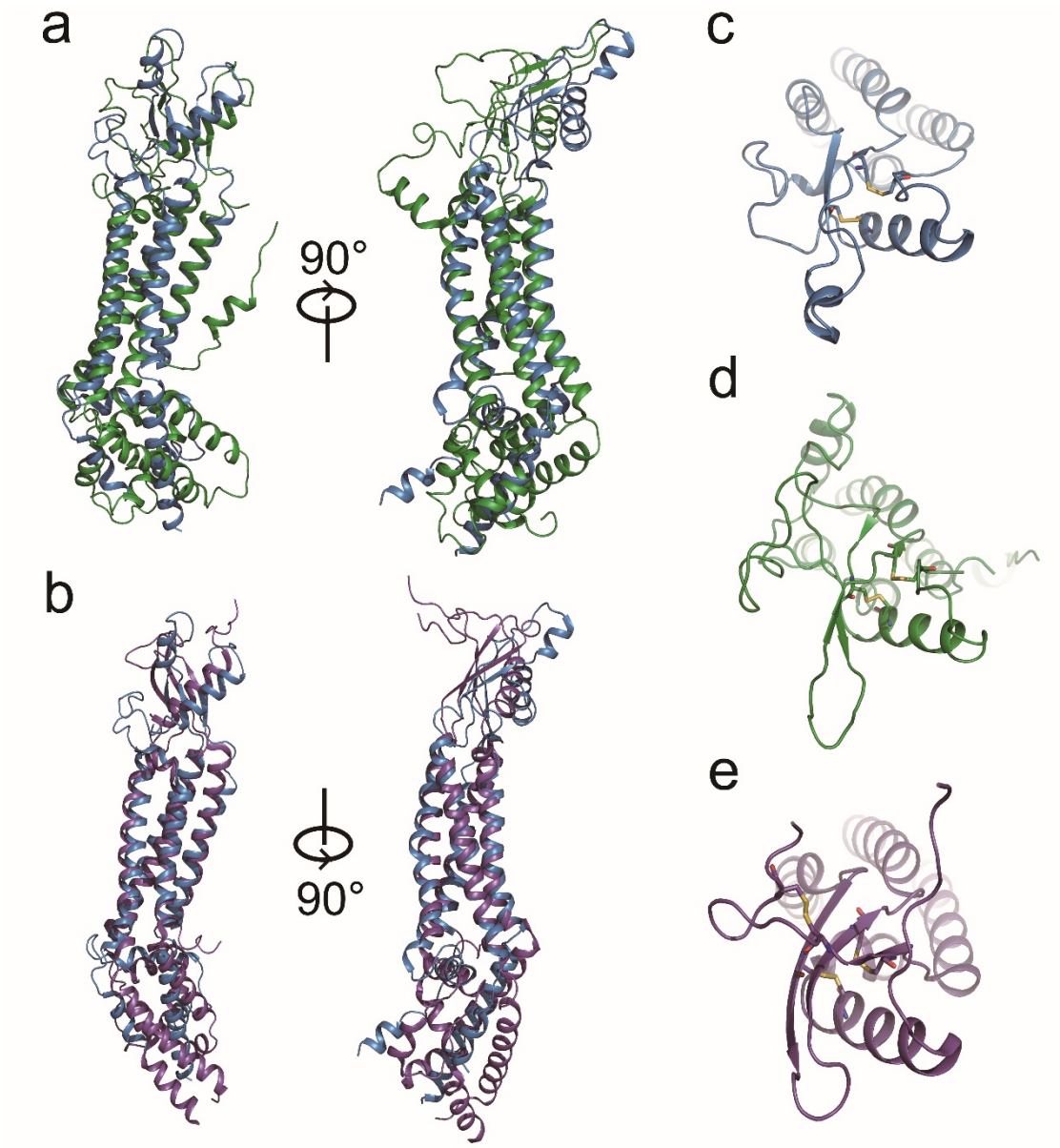

Figure S11. Structure comparisons between PANX1 and other large pore-forming channels. **a** Representation of a superposition of $PANX1_{EE}$ protomer and cINX6 (PDB: 5H1Q) protomer. PANX1 is shown in blue and cINX6 is shown in green. **b** Representation of a superposition of $PANX1_{EE}$ protomer and mLRRC8A (PDB: 6G8Z) protomer. PANX1 is shown in blue and mLRRC8A is shown in purple. **c,d,e** Zoom in views of conserved disulfate bonds in PANX1 **(c)**, cINX6 **(d)** or mLRRC8A **(e)**.

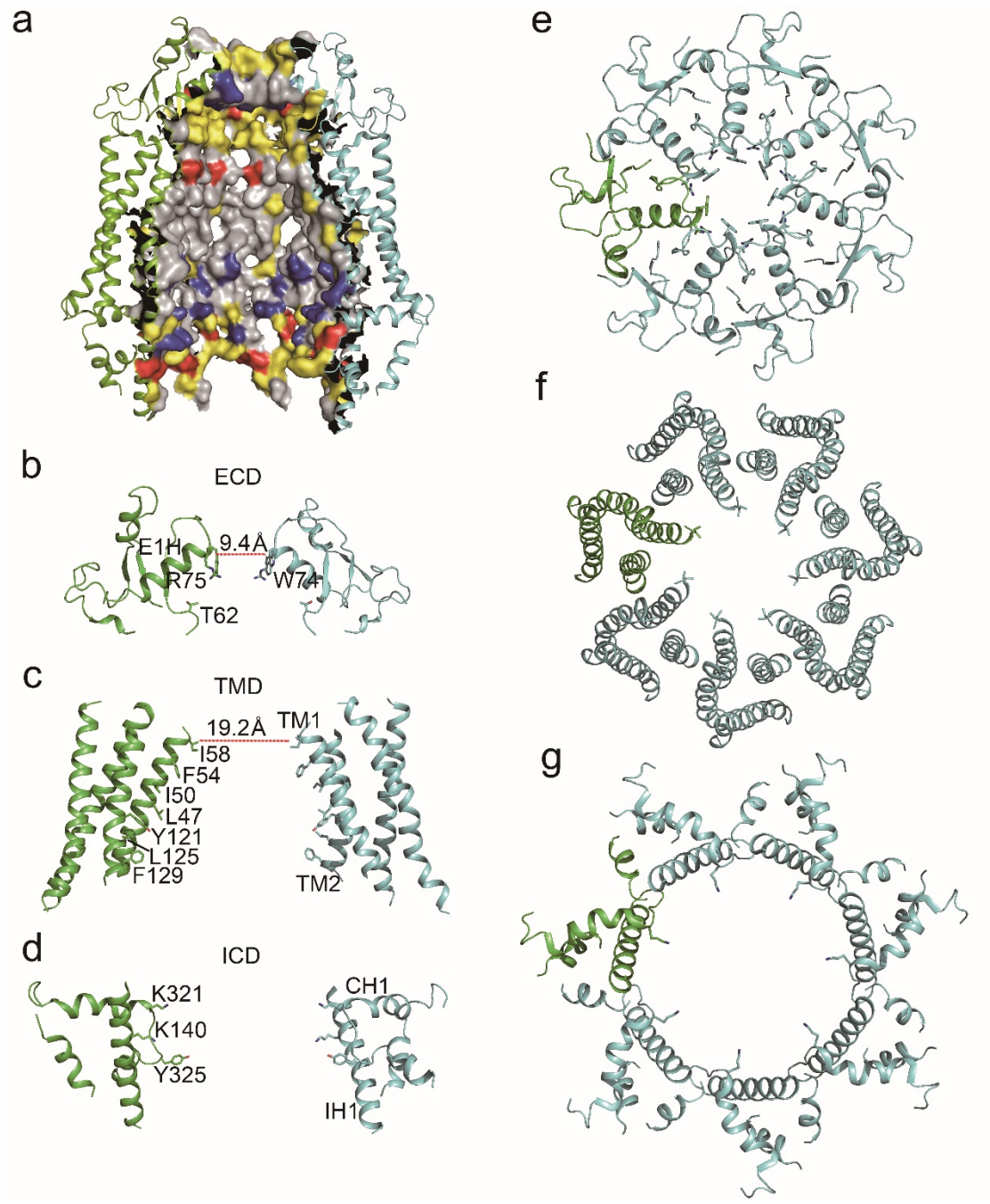

Figure S12. The pore organization of PANX1 channel. **a** Representative surface of the substrate conduction pathway view within the membrane. Two front subunits are removed and the residues are colored according to the electricity (positive charged, blue; negative charged, red; polar, yellow; non-polar, grey). **b,c,d** Zoom-in views of pore-forming domains and residues in ECD **(b)**, TMD **(c)** or ICD **(d)**, viewed parallel to the

plasma membrane. For clarity, only two subunits are shown. **e,f,g** Zoom in views of pore-forming domains and residues in ECD **(e)**, TMD **(f)** or ICD **(g)**, viewed extracellular side.

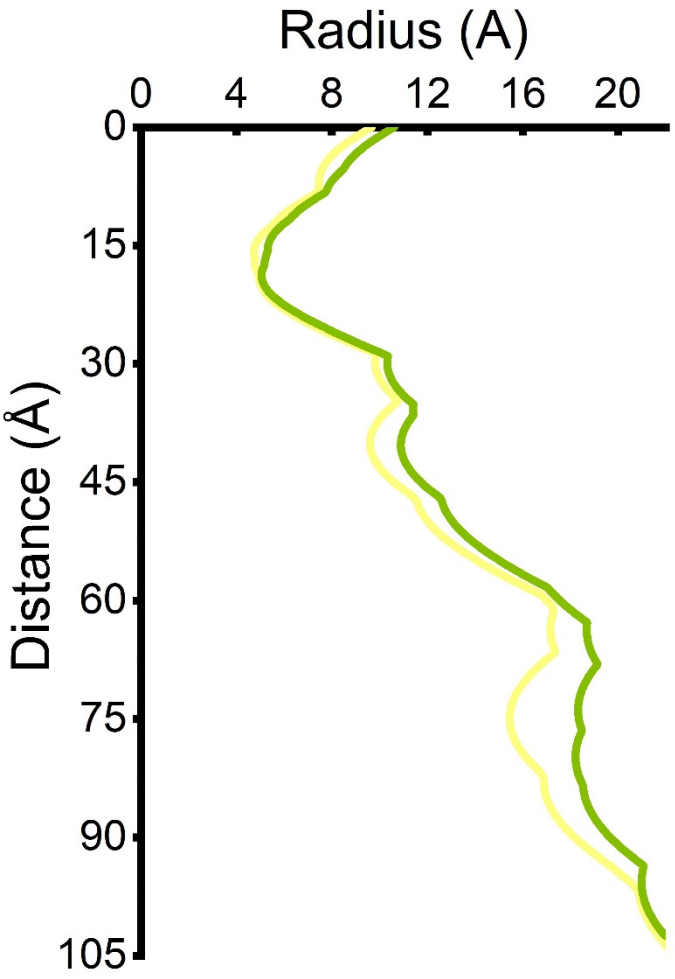

Figure S13. Channel pore comparison between $PANX1_{EE}$ and $PANX1_{WT}$. Representation of a comparison of pore radius of $PANX1_{EE}$ (yellow) and $PANX1_{WT}$ (green).